




Ultrasonic-Assisted Calcium Lignosulfonate Treatment of Titica Vine Fibers: Effects on Fiber and Composite Properties

Juliana dos Santos Carneiro da Cunha^{a*} , Ulisses Oliveira Costa^b , Michelle Souza Oliveira^a,
Lucio Fabio Cassiano Nascimento^a, Sergio Neves Monteiro^a 

^aInstituto Militar de Engenharia, Departamento de Engenharia e Ciências dos Materiais, Rio de Janeiro, RJ, Brasil.

^bUniversidade Federal Fluminense, Escola de Engenharia Industrial Metalúrgica de Volta Redonda, Programa de Pós-Graduação em Engenharia Metalúrgica, Volta Redonda, RJ, Brasil.

Received: April 19, 2025; Revised: October 19, 2025; Accepted: October 26, 2025

This research investigated the application of previously treated titica vine fibers (TVFs) as a reinforcing element in bio-based composites, aiming at the development of sustainable materials with better properties. The fibers were modified with calcium lignosulfonate (CaLS), a byproduct of the cellulose industry with potential compatibilizing properties in polymer composites. Surface treatments on natural fibers are essential to improve adhesion between the fibers and the polymer matrix, promoting a more efficient interface in the composite. Furthermore, they can reduce moisture absorption and eliminate impurities, resulting in increased mechanical properties and physical and chemical stability of the final material. Fourier transform infrared spectroscopy (FTIR) analysis confirmed characteristic vibrations of the fiber's main constituents, while X-ray diffraction (XRD) revealed a crystallinity index of 55.16% and a reduced microfibrillar angle (MFA) of 6.61°. The treated fibers exhibited a water absorption rate of 15.28% and a diffusion coefficient of $3.90 \text{ (mm}^2 \cdot \text{s}^{-1}) \times 10^{-4}$. Mechanical properties, assessed via Charpy and Izod impact tests, showed maximum absorbed energy values of $58.44 \pm 18.31 \text{ J/m}$ and $51.26 \pm 10.79 \text{ J/m}$, respectively. Scanning electron microscopy (SEM) revealed predominantly brittle fracture behavior. Despite moderate toughness, the treatment effectively reduced MFA, improving fiber structural characteristics.

Keywords: *Titica vine fiber, Composites, Calcium lignosulfonate, Surface treatment.*

1. Introduction

Given the growing importance of composite materials in engineering, they have transformed the construction, maritime, automotive, defense, aerospace and sports industries¹⁻³. With the search for sustainable alternatives to synthetic fibers, natural lignocellulosic fibers (NLFs) stand out as a promising solution, because of their high availability, low cost and biodegradability¹⁻³. In addition to meeting environmental concerns, NLFs offer a competitive strength-to-weight ratio^{4,5}, making them an attractive option for reinforcing new-generation composites. They compete with synthetic fibers, offering high-performance physical and mechanical properties, as well as being easier to manufacture^{6,7}.

The strength and properties of NLFs in composite materials are influenced by several factors, including fiber chemical composition, morphology, degree of crystallinity, moisture content, and fiber orientation in the matrix⁸⁻¹⁰. According to the literature¹¹, chemical treatments are especially efficient in removing considerable amounts of amorphous components such as waxes, pectin, hemicellulose, lignin and impurities

from the surface of fibers, by promoting the breakdown of hydroxyl groups. This process results in a significant increase in cellulose in relation to the amorphous constituents, thus improving the performance properties of natural fibers^{12,13}. In addition, the hydrophilic nature of NLFs, which opposes the hydrophobic character of many polymeric matrices, contributes to the weak fiber-matrix interfacial bond¹⁴⁻¹⁶. Surface modifications can increase fiber surface roughness^{11,17} enhancing mechanical interlocking with the matrix and improving interfacial adhesion. However, certain treatments may also reduce fiber crystallinity or increase hydrophilicity, potentially affecting mechanical performance and fiber-matrix compatibility. Understanding these trade-offs is crucial to optimizing fiber treatments for composite applications¹⁸.

Chemical treatments are widely used to enhance the adhesion between natural fibers and polymer matrices by modifying their surface chemistry and reducing amorphous constituents. Studies have shown that alkaline with NaOH¹⁹⁻²², silanes²³, pyrolysis²⁴ and benzoyl chloride treatments²⁵, for example, can enhance mechanical performance by increasing cellulose content and reducing lignin and hemicellulose fractions¹⁹⁻²⁵. However, the efficiency of such modifications depends on the treatment method and fiber type.

*e-mail: julianacunha@ime.ub.br

Associate Editor: Sandro Amico.

Editor-in-Chief: Luiz Antonio Pessan.

Regarding the modifying agents, it is interesting to explore treatments that use reagents from sustainable resources, in order to guarantee consistency in the use of NLFs as alternatives to materials derived from non-renewable sources²⁶. The wood refining industry has been an essential source for obtaining the main components of lignocellulosic materials (cellulose, hemicellulose and lignin), making it possible to separate these materials for the development of alternative chemical products derived from renewable sources²⁷. Lignosulphonates (LS) are by-products of pulp and paper production, through the sulphite pulping process of wood, in which the wood is digested at 140 - 170°C with an aqueous solution of a sulphite or bisulphite salt of sodium, ammonium, magnesium or calcium, in which several chemical events occur during the process²⁸. This procedure generates a black liquor, rich in lignin, carbohydrates and wood extractives. LS is extracted after dilution and filtration of the liquor to remove polymers and low molecular weight fractions. Figure 1 shows part of the structure of the calcium lignosulfonate (CaLS) used in this research and its effect on the morphological structure of Amazonian titica vine fibers (TVFs).

While previous studies have investigated the reinforcement of polymer composites with NLFs and various chemical treatments to improve fiber-matrix adhesion, this work introduces an innovative approach using CaLS, an abundant and renewable biopolymer derivative. Furthermore, compared to traditional treatments such as alkaline, silane and acetylation, it is non-toxic, does not generate hazardous waste, tends to better preserve the fiber's structural integrity and does not require expensive reagents or greater process control. Additionally, CaLS and the epoxy matrix used in

this study share functional groups similar to those found in NLFs such as hydroxyls (polar), hydrocarbons and aromatic rings (non-polar) and its application to the fiber surface can favor compatibility between the reinforcement and the matrix, improving interfacial adhesion¹⁶.

Ultrasonic impregnation enhances this process, promoting more uniform and effective penetration of CaLS into the fibers, thanks to cavitation and microbubbles generated by ultrasound²⁹, which increase reactivity and adhesion at the fiber-matrix interface. This innovative combination of chemical-mechanical treatments can contribute to the manufacture of materials with better performance and higher renewable content, enhancing the sustainability and functionality of natural fiber-based composites.

In this study, TVFs were modified for the first time using a combination of chemical (CaLS) and mechanical (ultrasonic bath) treatments. The ultrasonic process can disrupt fiber structure and potentially influence crystallinity and fiber-matrix interaction. Therefore, this study investigates the potential of CaLS treatment to modify the chemical, structural, physical and mechanical properties of TVFs, assessing its effects on crystallinity, microfibrillar angle, water absorption, and impact resistance when incorporated into epoxy composites. Using the FTIR technique, it was possible to evaluate the chemical interactions that occurred post-treatment. The crystallinity index (CI), as well as the microfibrillar angle (MFA), could be estimated using X-ray diffraction (XRD). The physical properties of the composites with treated fibers were measured using the water absorption test and determination of the diffusion coefficient. The Charpy and Izod impact tests made it possible to quantify

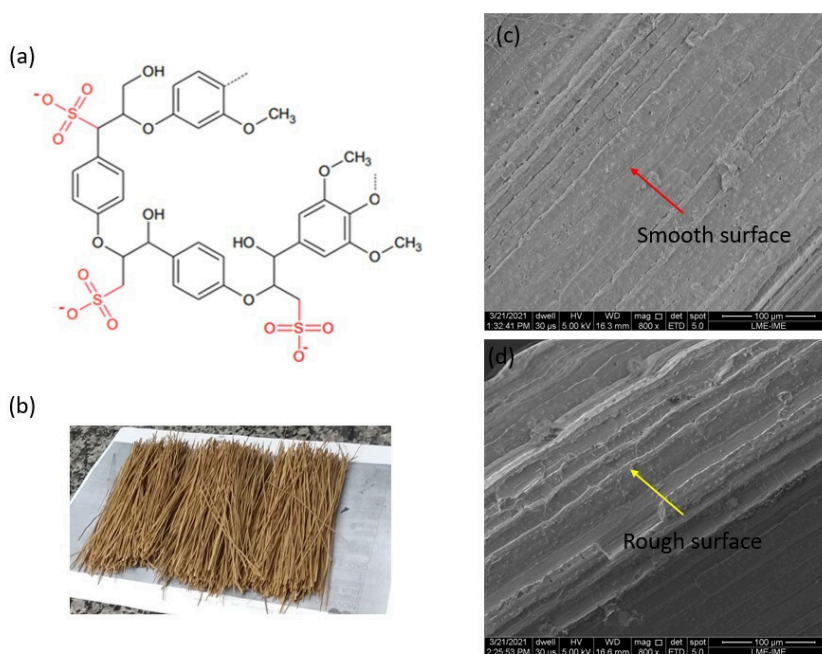


Figure 1. (a) Part of the chemical structure of CaLS; (b) TVFs; (c) SEM of the longitudinal surface of an untreated TVFs, 800x magnification; (d) SEM of the longitudinal surface of a TVFs after treatment with CaLS in an ultrasonic bath, 800x magnification.

the mechanical properties. In addition, the fracture surfaces were analyzed using SEM in order to elucidate the fracture mechanisms acting on the composites. This research explores, for the first time, the use of CaLS in an ultrasonic bath as a renewable compatibilizer for TVFs in epoxy composites.

2. Experimental Procedures

2.1. Materials

The TVFs were purchased in the form of thick roots from a local market in the city of Boa-vista, state of Roraima, northern Brazil. The material was mechanically cut into stalks and subsequently immersed in water for 24 hours to facilitate fiber extraction using a manual blade.

The 99% purity CaLS used for fiber treatment was supplied by Auro's Química (São Paulo, Brazil). Initially, the fibers were washed twice: first with deionized water at 70 °C for 1 hour, and then with a mixture of 99.4% ethyl alcohol (Prolink Química, São Paulo, Brazil) and acetone P.A. (95:5 v/v) from BHerzog (Rio de Janeiro, Brazil), under the same conditions as the first wash.

For every 1 L of deionized water, 50 g of CaLS was dissolved, thus obtaining a 5 wt.% solution of CaLS, in which 100 grams of fibers were immersed. At room temperature, impregnation was carried out in an ultrasonic bath. The equipment used was a Soniclean ultrasonic cleaner from SANDERS, using a frequency of 40KHz, for a period of 1 hour. After this stage, they were removed and dried in an oven at 60°C for 24 hours until they reached a constant weight.

The resin used as the matrix for the composites was diglycidil ether of bisphenol A (DGEBA) hardened with triethylene tetramine (TETA). The proposed stoichiometry was 13 parts hardener to 100 parts resin by weight. The

manufacturer of the product is Dow Chemical from Brazil, and it is supplied by the distributor Epoxyfiber Ltda.

2.2. Composite processing

The composites of 10, 20, 30 and 40 vol% TVFs treated with CaLS in an ultrasonic bath (TVFs-CaLS-UB) were prepared using the Hand Lay-Up process, in which a compression force of 5 MPa was applied in a Sky, Brazil hydraulic press at room temperature for 24 hours, as shown in Figure 2.

The 15 cm long fibers were arranged in a preferentially aligned direction in a metal mold with an internal volume of 214.2 cm³ (dimensions 15 x 12 x 1.19 cm). For the manufacture of the composites, 0.50 g/cm³ was adopted as the average density for TVFs²¹ and 1.11 g/cm³ for epoxy resin³⁰.

2.3. Fourier transform infrared spectroscopy (FTIR)

The FTIR analysis was carried out on a Shimadzu IRPrestige-21 (Tokyo, Japan). The fibers were ground to a powder, which made it possible to produce a tablet with KBr. The scan was carried out over a spectral range of 4000 to 400 cm⁻¹, generating transmittance spectra (%) as a function of wavenumber (cm⁻¹).

2.4. X-ray diffraction (XRD)

The XRD analysis was carried out on PANalytics equipment, model X'Pert PRO, with Cobalt radiation (1.789 Å), 40 mA x 40 kV power and a scan range of 10 to 75°. The crystallinity index (CI) of TVFs-CaLS-UB was calculated according to the methodology developed by Segal et al.³¹, which uses the maximum intensity of the amorphous (101) and crystalline (002) peaks, represented by I_{am} and I_{cris},

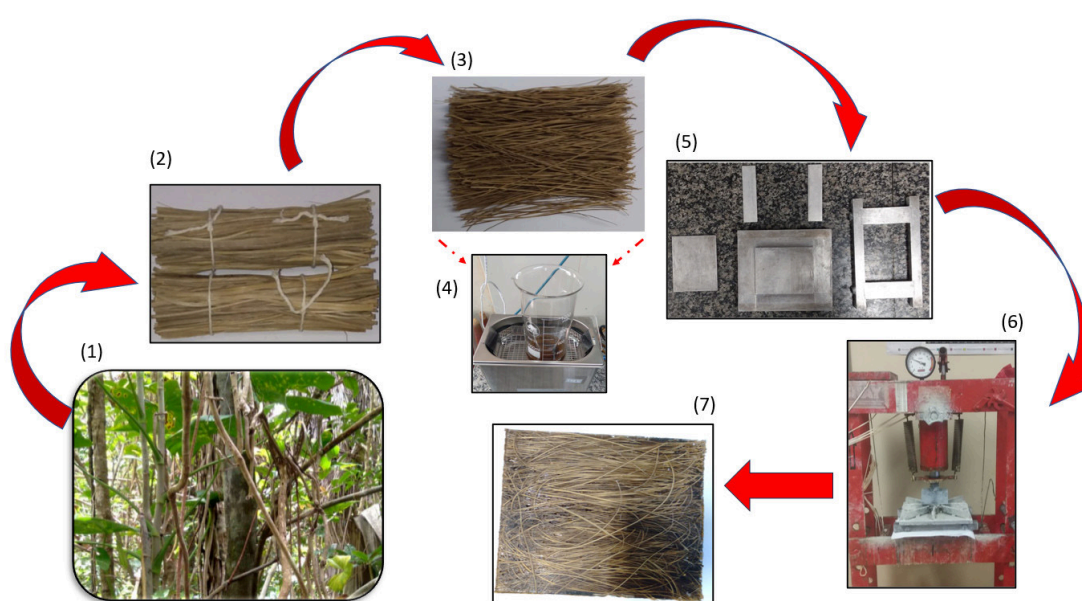


Figure 2. Schematic diagram of the composite manufacturing process. (1) TVFs source plant; (2) TVFs as splints; (3) TVFs 15 cm long; (4) dissolution of CaLS for subsequent immersion of TVFs; (5) mold where the fibers will be accommodated and impregnated with resin; (6) hydraulic press; (7) manufactured composite plate.

respectively. The CI value of the post-treated fiber was estimated from EQ. (1).

$$CI = \frac{I_{\text{crys}} - I_{\text{am}}}{I_{\text{crys}}} * 100 \quad (1)$$

The microfibrillar angle (MFA) was measured using the methodology proposed by Donaldson³² and Sarén and Serimaa³³ through the deconvolution of the crystalline cellulose peak (002), in which the Gauss curves and their first and second order derivatives are provided. Using OriginPro 8.5 software, the baseline of the diffractogram was removed and the peak (002) was isolated. The Gaussian curve of this peak was fitted and two other curves associated with their derivatives were generated from it. With this procedure, it is possible to obtain the “T” parameter, which refers to half the distance between the intersections of the tangents at the inflection points of the peak curve (002) and the baseline. EQ. (2) lists the “T” parameter for calculating the MFA of the TVFs-CaLS-UB.

$$MFA = -12.19T^3 + 113.67T^2 - 348.40T + 358.09 \quad (2)$$

2.5. Water absorption and diffusion coefficient

The water absorption test on the composites with treated fibers was carried out in accordance with ASTM D570-98³⁴. The test results were calculated using the difference in weight of the samples, according to EQ. (3).

$$\%WA = \frac{M_{\text{final}} - M_{\text{initial}}}{M_{\text{initial}}} \quad (3)$$

Where: %WA - Percentage of water absorption; M_{initial} - mass of the specimen before immersion; M_{final} - mass of the specimen after immersion.

Based on Fick's law, the behavior of diffusion kinetics was evaluated. In the case of polymeric materials, diffusion can be grouped into three types, as reported in previous research³⁵⁻³⁷. Synthetically, this classification addresses the relative mobility between the penetrant and the polymer

segments. The different categories can be distinguished by fitting the experimental values to EQ. (4):

$$\log \frac{M_t}{M_\infty} = \log(k) - n \log(t) \quad (4)$$

Where: M_t - moisture content at time t ; M_∞ - moisture content at equilibrium; k and n - constants.

To analyze the diffusion coefficient (D), we used the theoretical model provided by Fick's law, which is included in equation (4):

$$\frac{M_t}{M_\infty} = \frac{4}{L} * \left(\frac{D}{\pi} \right)^{0.5} t^{0.5} \quad (5)$$

Where: L - sample thickness.

2.6. Charpy and izod impact tests

The Charpy and Izod impact tests were carried out in a Pantec pendulum apparatus, model XC-50, Charpy and Izod configuration, operating with a 22 J hammer, in accordance with ASTM D6110-18³⁸ and ASTM D256-10³⁹, respectively. For the Charpy tests, a minimum of eight samples per volume fraction were tested, while for the Izod tests, at least twelve samples were used. Figure 3 presents the composite specimens produced.

2.7. Statistical validation

The energy absorbed by the test specimens was statistically evaluated and validated in terms of reliability and significance using the Weibull distribution and analysis of variance (ANOVA), together with the Tukey test.

2.8. Scanning electron microscopy (SEM)

This technique was used to investigate the morphology of the fracture surface after mechanical testing. Its main purpose is to understand the failure mechanisms acting on the material and to assess the quality of the interface between the fiber and the polymer matrix. The microscopic aspects of the fractured composites after the Charpy and Izod impact

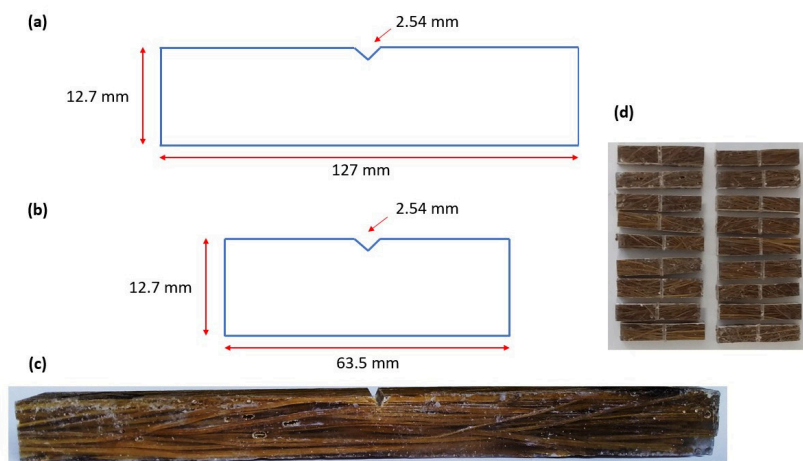


Figure 3. (a, b) Standard dimensions of Charpy and Izod specimens, respectively; (c) Charpy specimen produced; (d) Izod specimens made.

tests were analyzed on a Quanta FEG 250 microscope FEI, Switzerland, operating with secondary electrons and voltages of up to 5 kV. All samples were sputter coated with gold using a LEICA EM ACE600.

3. Results and Discussion

3.1. Fourier transform infrared spectroscopy (FTIR)

Figure 4 shows the FTIR spectra of the TVFs after treatment, represented by TVFs-CaLS-UB and Calcium Lignosulfonate, CaLS, compared to the untreated fiber, TVFs-U, studied previously⁴⁰. Through these it is possible to identify absorption bands that correspond to specific molecular vibrations, making it possible to identify different functional groups associated with the main constituents of NLFs and responsible for their properties.

Table 1 summarizes the main absorption bands observed in the TVFs-CaLS-UB spectrum. No significant changes were observed between the spectra of the fibers before and after treatment. This is related to the low quantity of CaLS deposited on the surface of the TVFs, which is considered low in relation to its integral composition. Thus, the signals from the fiber's original lignin may overlap with the signals from the CaLS deposited on it.

However, it is possible to notice bands whose relative proportions have changed. Some of them are at wavelengths of 2924 cm^{-1} and 1651 cm^{-1} , which are characteristic of the addition of methoxyl groups during the sulfonation reaction and axial deformation of the C=C bonds of the aromatic ring, respectively. The brief expansion of these bands, and consequently the increase in their areas, is probably related to the presence of CaLS. Another similar case occurs at 1041 cm^{-1} , which may be associated with the insertion of the $-\text{SO}_3$ group. Finally, the band at 834 cm^{-1} of the untreated fiber, TVFs-U, is noteworthy because after treatment it becomes imperceptible. It is also not shown in the CaLS spectrum. As this band is related to the stretching of functional groups belonging to units present in lignin, it can be inferred that the treatment reduced this constituent.

Although the FTIR spectrum of CaLS-treated fibers reveals no significant changes compared to untreated fibers, variations in specific bands suggest the presence of the modifying agent and indicate possible chemical interactions with the fiber surface. The observed changes in the relative intensities of bands associated with methoxyl, sulfonate,

and aromatic bonds, as well as the disappearance of bands linked to the original lignin, reinforce the hypothesis that CaLS treatment promotes specific changes in the surface composition of the fibers, albeit at low concentrations.

3.2. X-ray diffraction (XRD)

The diffraction pattern was analyzed using OriginPro 8.5 software by means of computational data processing. Figure 5 shows the diffractogram obtained for the TVFs-CaLS-UB.

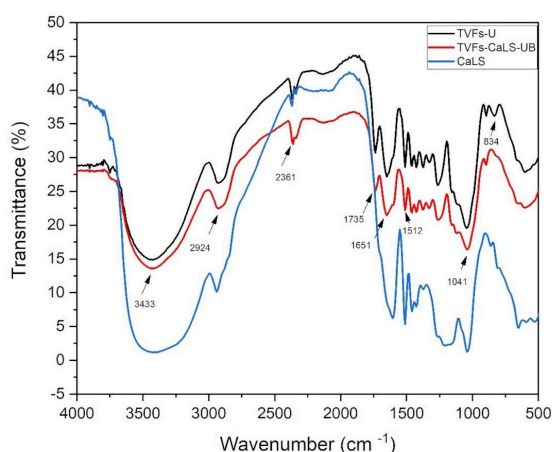


Figure 4. TVF after treatment, TVFs-CaLS-UB compared to untreated fiber, TVFs-U.

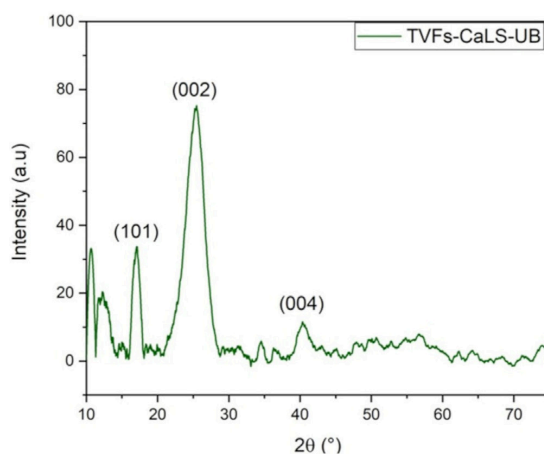


Figure 5: XRD pattern of the TVFs-CaLS-UB fibers.

Table 1. Main FTIR absorption bands for the TVFs after treatment with Calcium Lignosulfonate in an ultrasonic bath (TVFs-CaLS-UB).

Position cm^{-1}	Band assignment	Reference
3450 – 3400	O-H bond (Cellulose, Hemicellulose, Lignin and Lignosulfonates)	41-43
2960 – 2830	Stretching of C-H and R-O-CH ₃ groups (Cellulose, Hemicellulose, Lignin and Lignosulfonates)	44-46
2368 - 2337	C-H Stretch (Cellulose and Hemicellulose)	44
1735	C=O bond (Lignin and Hemicellulose)	42,47
1655 – 1455	CH ₃ asymmetric deformation; C=C stretching (aromatic ring) (Lignin and Lignosulfonates)	48-50
1041	C-H/C-O and C-C stretching (Cellulose, Hemicellulose, Polysaccharides and Lignosulfonates)	44,46,50,51
834	Out of plane C-H stretching of Guaiacyl, Syringyl and p-hydroxyphenyl units (Lignins)	52

Figure 5 presents the diffractogram after normalizing the baseline, to make it easier to see the relevant peaks. The fibers analyzed showed typical semi-crystalline behavior, with the (101), (002) and (004) planes standing out. To measure the crystallinity index, Equation (1) was used, which relates the interference intensity in the (002) plane corresponding to the $2\theta = 25.47^\circ$ peak and the scattering of the amorphous region in the (101) plane, referring to the peak at $2\theta = 17.08^\circ$.

The crystallinity index (CI) of the TVFs after treatment was 55.16%, indicating a structural reorganization of the fibers. While a decrease of 29.6% was observed compared to untreated fibers, this transformation suggests increased fiber flexibility and potential improvements in fiber dispersion within polymer matrices. Such changes may enhance composite processing and energy dissipation mechanisms under mechanical loading^{31,40}. According to Flannigan et al.⁵³, as ultrasound propagates through a liquid medium, microbubbles form and collapse, an event called cavitation. When a sound wave passes through a liquid, regions of compression (positive pressure) and rarefaction (negative pressure) are created. If the negative pressure is high enough, a cavity or bubble can be formed in the liquid from the nucleus of gases present inside the fluid. The bubbles are distributed throughout the liquid, grow to a critical size, become unstable and collapse⁵⁴. When cavitation occurs close to a solid surface, the collapse is asymmetrical and

favors the formation of liquid jets with high velocity towards the surface of the solid, hitting it with considerable force. The resulting collisions can cause changes to the surface, composition and morphology⁵⁵.

Since cellulose determines the crystallinity of NLFs, this result may indicate that the ultrasonic irradiation used in the presence of CaLS allows for the disaggregation of fiber bundles and the penetration of the species present in the medium ($\text{Ca}^+/\text{H}_2\text{O}$) into the crystalline domains, as occurs in mercerization⁵⁶, a fact that contributed to the reduction in crystallinity of TVFs after treatment. This same behavior was evidenced by Oliveira et al.²⁶ when researching sisal fibers treated with sodium lignosulfonate under different conditions, including ultrasound irradiation.

Like the CI, the orientation of the microfibrillar angle (MFA) is also mentioned as one of the factors responsible for improving the mechanical properties of NLFs^{57,58}. Using the diffraction pattern obtained, as shown in Figure 5, it is possible to estimate the MFA of the TVFs-CaLS-UB fibers. The peak attributed to the crystalline phase in the plane (002) was isolated, and based on mathematical methods, the MFA of the TVFs after surface modification was measured. Figure 6 shows the graphs associating the peaks (002), adjusted by a Gaussian and their first and second order derivatives.

The microfibrillar angle (MFA) of the treated fibers decreased to 6.61° , a 16.8% reduction compared to untreated samples⁴⁰. This value places the modified TVFs among the lowest MFA values reported for natural fibers (Table 2), indicating a more aligned fibrillar structure, which is often associated with increased stiffness and enhanced load transfer in composite applications, which may have induced structural modifications, affecting both the morphological surface (Figure 1d) and the composition (Table 2) due to the presence of CaLS. Notably, the CaLS-treated TVF exhibited the lowest microfibrillar angle reported in the literature, which could significantly enhance its mechanical properties.

The MFA, which can be defined as the angle formed by the microfibrils in relation to the longitudinal axis of the fiber, has a direct influence on the mechanical properties of NLFs, such as toughness and rigidity. The lower the MFA, the more resistant and rigid the fibers tend to be. On the other hand, high angles tend to increase ductility and predisposition to fracture⁶⁵. In addition, varying this angle can affect other properties such as air permeability and moisture absorption⁶⁶.

The result obtained for TVFs after treatment, despite its decrease in CI, places it on the same level as other NLFs,

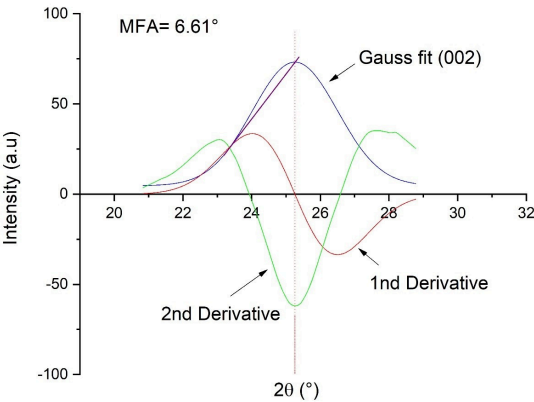


Figure 6. Microfibrillar angle of TVFs after treatment with CaLS in an ultrasonic bath, TVFs-CaLS-UB.

Table 2. Crystallinity index and microfibrillar angle of CaLS-treated (TVFs-CaLS-UB) and untreated (TVFs-U) liana fibers in relation to other NLFs.

Fiber	CI (%)	MFA (°)	Reference
TVFs-CaLS-UB	55.16	6.61	PW
TVFs-U	78.3	7.95	40
Cyperus malaccensis	62.47	7.36	59
Mendong Grass	58.60	22.90	60
Kenaf	44.3	7.10	61
Acacia Pennata	46.52	19.67	62
Heteropogon contortus	54.10	14.53	63
Sida cordifolia stem	56.92	9.50	64

PW – Present Work

including those already established in the literature, such as kenaf. In addition, this was compensated for by the fact that its MFA was the lowest of all the other NLFs (Table 2) and was able to induce an improvement in its mechanical resistance properties.

3.3. Water absorption and diffusion coefficient

Figure 7 presents the water absorption behavior of the composites containing 40 vol% TVFs treated with CaLS in an ultrasonic bath (TVF40-CaLS-UB), compared to untreated fiber composites (TVF40-U). After 504 hours of immersion, the water absorption of TVF40-CaLS-UB composites was 15.28%, showing a moderate increase relative to untreated samples (13.77%).

This trend aligns with previous studies on lignosulfonate-treated fibers¹⁶, where slight increases in water absorption have been attributed to modifications in fiber surface chemistry. The ultrasonic bath may have influenced fiber morphology and microstructure, contributing to enhanced fiber-matrix interactions while also increasing the number of hydroxyl groups available for moisture adsorption. However, such effects can be mitigated through complementary treatments, such as additional hydrophobic coatings or alternative processing conditions.

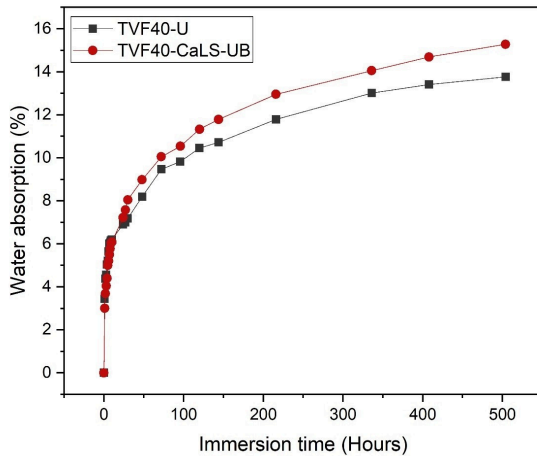


Figure 7. Water absorption curve for composites with 40 vol% of fibers treated with CaLS in an ultrasonic bath (TVF40-CaLS-UB) compared to composites with the same percentage of fibers, but without any treatment (TVF40-U).

Using the data obtained in the water absorption test, Fick's law (Eq. 4 and 5) was applied to investigate the water diffusivity process in the composites with TVFs-CaLS-UB. Table 3 presents the values of the diffusion coefficient (D) and the parameter "k".

The diffusion coefficient (D) values confirm that, while the treated fibers exhibited slightly higher water mobility within the composite ($3.900 \times 10^{-4} \text{ mm}^2 \cdot \text{h}^{-1}$ vs. $3.770 \times 10^{-4} \text{ mm}^2 \cdot \text{h}^{-1}$ for untreated), the material's overall structural integrity remains preserved. This suggests that with further processing refinements, CaLS-treated fibers could be optimized for enhanced moisture resistance while retaining their mechanical benefits.

The increase in D for composite samples with treated fibers compared to those with untreated fibers indicated a material more prone to penetration of water molecules and with greater ability to move within the composite. The variation in the "k" value is related to the strong affinity of water with the composite, showing that the fibers after treatment were not as well protected by the matrix and that their impregnation by epoxy was impaired due to poor anchoring justified by their more hydrophilic character that they presented post-treatment.

Despite this slight increase in D and "k" compared to the untreated TVF composites, these values are quite satisfactory compared to the polyester/pandanus fascicularis lam (30%) systems treated with 3% NaOH⁶⁷, polyester/pandanus fascicularis lam (30%) without treatment⁶⁷, and polyester/palf (40%)⁶⁸. On the other hand, the untreated polyurethane/tucum (50%)⁶⁹ and untreated polyurethane/mallow (50%)⁶⁹ composites obtained the best performances in similar tests. Therefore, as can be observed from the literature records, the TVF40-CaLS-UB composites become a viable alternative for applications that require moisture resistance.

3.4. Charpy and izod impact tests

Figure 8 presents the results of Charpy and Izod average absorbed impact energy (E_{abs}) of the composites manufactured with TVFs-CaLS-UB in the fractions of 10 – 40 vol% of NLFs. In addition, a comparative study was carried out with the composites of untreated fibers¹⁶, the control group (plain epoxy)¹⁶ and with the composite of 40 vol% of TVFs with CaLS under heating and magnetic stirring (TVF40-CaLS-70°C)¹². The Charpy impact test (Figure 8a) revealed a progressive increase in absorbed energy (E_{abs}) with the addition of fibers, reinforcing the role of TVFs in enhancing composite toughness. Although the absolute values for the

Table 3. Diffusion coefficient (D) values and "k" parameter.

Samples	D ($\text{mm}^2 \cdot \text{h}^{-1}$) $\times 10^{-4}$	k	Reference
TVF40-CaLS-UB	3.900	0.997	PW
TVF40-U	3.770	0.975	¹⁶
Polyester/pandanus fascicularis lam (30%) - 3% NaOH	25.23	-	⁶⁷
Polyester/pandanus fascicularis lam (30%) untreatment	31.65	-	⁶⁷
Polyester/palf (40%) untreated	7.20	1.193	⁶⁸
Polyurethane/tucum (50%) untreatment	0.0013	0.13	⁶⁹
Polyurethane/mallow (50%) untreatment	0.00057	1.34	⁶⁹

PW – Present Work

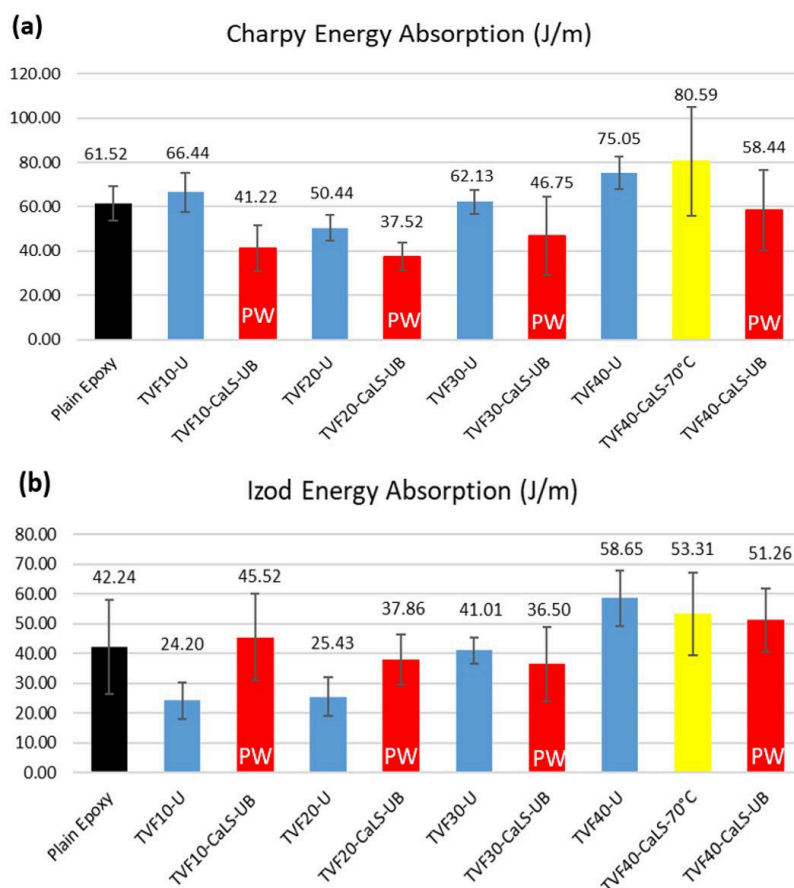


Figure 8. Variation of the impact energy absorbed by the composites manufactured with TVFs-CaLS-US in the fractions of 10 – 40 vol% of NLFs compared to those without treatment and treated with TVFs modified with CaLS at 70 °C under magnetic stirring (TVF40-CaLS-70°). PW – Present Work

CaLS-treated fibers (TVF40-CaLS-UB) were slightly lower than those of untreated fibers (TVF40-U) and those treated at 70 °C (TVF40-CaLS-70°C), the differences were within an expected range for chemically modified natural fibers.

Notably, the Charpy impact resistance of the TVF40-CaLS-UB composites remained comparable to plain epoxy, with only a 5% difference, indicating that the treatment preserved the matrix integrity while maintaining a reinforcing effect. The maximum value obtained in the Charpy test in this study (58 J/m) exceeds the results recorded for polyester composites with curaua fiber treated with 10% and 0.1% NaOH (38 and 27 J/m, respectively)⁷⁰, and is comparable to the performance of the linear low-density polyethylene system with sisal treated with a 3% maleic anhydride-grafted polyethylene solution (60 J/m)⁷¹. However, in both cases in the literature, the composites with untreated fibers presented superior performance — a trend that was also observed in the present investigation.

These results suggest that further adjustments in processing conditions, such as optimizing fiber dispersion and improving interfacial adhesion, as well as exposure time and functionalizing agent concentration, could enhance the energy dissipation mechanisms, unlocking the full potential of CaLS-treated fibers in impact-resistant applications

The results of the Izod test (Figure 8b) show that there was an increase in energy absorption when adding 40 vol% of fibers treated in an ultrasonic bath. When compared to pure epoxy, the TVF40-CaLS-UB group had a 21.3% increase in this property. However, again these samples (TVF40-CaLS-UB) presented lower values compared to TVF40-U and TVF40-CaLS-70°C. This difference represents a drop of 14.4% and 4%, respectively.

To confirm the effect provided by the treatment of TVFs-CaLS-UB in the 10–40 vol% NLFs composites, the Charpy and Izod impact energy absorption property was statistically analyzed by the Weibull method. Furthermore, the standard deviation values of the compositions may compromise the degree of certainty regarding whether the CaLS treatment in an ultrasonic bath acted or not as reinforcement in the matrix, as well as whether they were effective. Thus, analysis of variance (ANOVA) and Tukey test were performed to verify the occurrence of significant difference between the Charpy and Izod absorbed energy results for the plain epoxy, TVF40-U, TVF40-CaLS-70°C and TVF40-CaLS-UB groups. The choice is justified by the fact that plain epoxy was the control group and the 40 vol% fractions stood out in the tests.

3.5. Statistical validation

Table 4 shows the Weibull parameters (β e R^2), in addition to the characteristic unit θ . The Weibull modulus β or shape parameter controls the variation of the results and provides an assessment of the homogeneity of the material. R^2 values reflect the statistical reliability of the results achieved. The parameter θ refers to an estimate of whether the material analyzed presents a certain property.

Based on the values shown in Table 4, it is observed that, for both tests, the TVF30-CaLS-UB and TVF40-CaLS-UB composites tended to reveal lower β , that is, a greater variation in the values, which could also be verified by the greater standard deviation observed in these groups. The exception occurs only for the TVF40-CaLS-UB Izod samples, in which the greater homogeneity may have been the result of factors related to the efficiency of the treatment in this set of fibers, such as: greater removal of impurities, greater pore opening and reduction in water absorption capacity.

The parameter θ , as expected, followed the same pattern as the E_{abs} measured directly in the test. This index indicates that 63.2% of the samples in each group should present E_{abs} values corresponding to θ . The statistical precision coefficient R^2 showed high representativeness and was within a statistically acceptable reliability range (> 0.83). This result allows us to state that of the groups evaluated, a maximum of 17% of the samples cannot be justified by the Weibull mathematical model.

Table 5 presents the ANOVA of the Charpy and Izod impact resistance results for samples from the control group (plain epoxy) and 40 vol% composites with untreated and treated TVFs. The data in Table 5 indicate that the hypothesis of equality between the Charpy and Izod absorbed energy values is rejected with a 95% confidence level, since $F_{cal} = 3.43$ and 3.46 are higher than $F_{critical} = 2.95$ and 2.82 , respectively.

To verify which group presented better resistance to Charpy and Izod impact, the Tukey test was applied to

Table 4. Weibull parameters for Charpy and Izod impact resistance of TVFs-CaLS-US composite.

Sample	Charpy			E_{abs} (J/m)	Standard Deviation	Izod			E_{abs} (J/m)	Standard Deviation	Reference
	β	θ	R^2			β	θ	R^2			
TVF10-CaLS-UB	3.61	44.49	0.99	41.22	10.17	3.34	50.27	0.94	45.52	14.71	PW
TVF20-CaLS-UB	5.02	39.49	0.91	37.52	6.41	4.78	41.31	0.93	37.86	8.42	PW
TVF30-CaLS-UB	2.77	51.72	0.89	46.75	17.65	3.49	39.29	0.94	36.50	12.50	PW
TVF40-CaLS-UB	3.51	63.87	0.94	58.44	24.53	5.14	54.76	0.96	53.31	10.79	PW
Plain Epoxy	6.86	61.41	0.98	61.52	7.89	3.03	46.31	0.83	42.24	15.91	16
TVF40-U	5.80	74.67	0.96	75.05	7.32	4.99	61.02	0.92	58.65	9.26	16
TVF40-CaLS-70°C	3.40	88.5	0.94	80.59	24.53	4.27	59.52	0.91	53.31	13.89	16

PW – Present Work

Table 5. ANOVA for the absorbed impact energy Charpy and Izod of plain epoxy and 40 vol% composites with untreated and treated TVFs.

Variation Causes	Plain epoxy, 40 vol% treated and untreated (Charpy)					Plain epoxy, 40 vol% treated and untreated (Izod)				
	SS	DF	MS	F_{calc}	$F_{critical}$	SS	DF	MS	F_{calc}	$F_{critical}$
Treatment	2706.45	3	902.15	3.43	2.95	1680.68	3	560.23	3.46	2.82
Residue	7368.57	28	263.16			7130.42	44	162.05		
Total	10075.02	31				8811.10	47			

Table 6. HSD measured by Tukey's test for the absorbed Charpy impact energy of plain epoxy and 40 vol% composites with untreated and treated TVFs.

Sample	Plain Epoxy	TVF40-U	TVF40-CaLS-70°C	TVF40-CaLS-UB
Plain Epoxy	0.00	-13.53	-19.07	3.08
TVF40-U	13.53	0.00	-5.54	16.61
TVF40-CaLS-70°C	19.07	5.54	0.00	22.15
TVF40-CaLS-UB	-3.08	-16.61	-22.15	0.00

Table 7. HSD measured by Tukey's test for the absorbed Izod impact energy of plain epoxy and 40 vol% composites with untreated and treated TVFs.

Sample	Plain Epoxy	TVF40-U	TVF40-CaLS-70°C	TVF40-CaLS-UB
Plain Epoxy	0.00	-16.40	-11.07	-9.02
TVF40-U	16.40	0.00	5.33	7.38
TVF40-CaLS-70°C	11.07	-5.33	0.00	2.05
TVF40-CaLS-UB	9.02	-7.38	-2.05	0.00

compare individual performance with a 95% confidence level. Tables 6 and 7 present the values of the honest significant difference (HSD) obtained by the Tukey test for the Charpy and Izod tests, respectively.

The calculated HSD for the Charpy test was 22.14 J/m, and differences greater than this value are considered significant. The data in Table 6 indicate that the Charpy impact strength of the TVF40-CaLS-70°C composite was indeed greater than that of TVF40-CaLS-UB, and that there was no significant difference between the plain epoxy, TVF40-U, and TVF40-CaLS-70°C, since the difference between the means did not exceed the calculated HSD. For the Izod test, the calculated HSD was 7.24 J/m. The values in Table 7 showed that the Izod impact strength of the TVF40-CaLS-US composite was superior to that of plain epoxy but inferior to that of TVF40-U. Furthermore, no significant difference was observed between TVF40-CaLS-UB and TVF40-CaLS-70°C.

3.6. Scanning electron microscopy (SEM)

The increase in impact resistance observed as fibers were added to the composites may be related to the fracture mechanisms involved. Furthermore, this same explanation can be applied to justify the reduced toughness of TVF40-CaLS-UB samples when compared to untreated ones. To validate and deepen the analysis on the evolution of fracture mechanisms in the evaluated materials, Figures 9 and 10 show the fracture surfaces of the samples treated with CaLS in an ultrasonic bath (TVF10-CaLS-UB and TVF40-CaLS-UB), in the Charpy and Izod tests, respectively.

In Figures 9a and 10a, a completely fragile type of fracture can be seen, due to the strong presence of “river marks” on the impact surface of the samples. Furthermore, another failure mechanism frequently found for these composites was matrix fracture, which often occurred catastrophically, as there were few regions filled with fibers that could

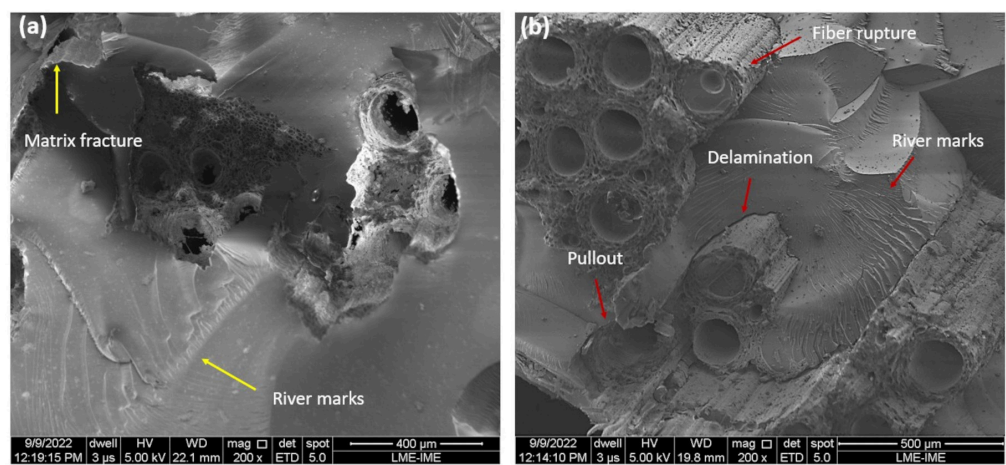


Figure 9. SEM of fracture surfaces of the Charpy tested samples. (a) TVF10-CaLS-UB composites, 200x magnification and (b) TVF40-CaLS-UB, 200x magnification.

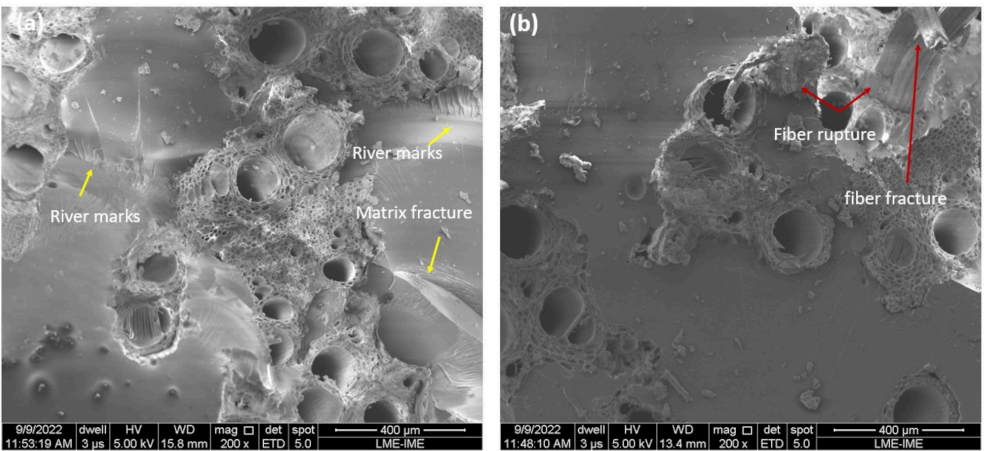


Figure 10. SEM of fracture surfaces of the Izod tested samples. (a) TVF10-CaLS-UB composites, 200x magnification and (b) TVF40-CaLS-UB, 200x magnification.

serve as a barrier to crack propagation. On the other hand, more complex fracture mechanisms were activated in the TVF40-CaLS-UB composites (Figures 9b and 10b), such as fiber rupture and fracture, delamination's and pullout. Although there was still the presence of "river marks", a significant decrease was noticeable across the entire surface. The presence of these new mechanisms explains the more efficient performance of these samples when compared to those with a lower percentage of fibers, as these can provide an additional free surface with the capacity to increase the tenacity of the composites. These findings align with previous studies^{59,72,73}, which observed variations in impact energy absorption in composites reinforced with different natural fibers. Such variations are often attributed to differences in fiber morphology, surface modification, and fiber-matrix interaction. The observed trend suggests that further optimization of treatment parameters, such as processing conditions and fiber dispersion, could enhance the energy dissipation mechanisms, potentially improving the impact resistance of CaLS-treated composites.

Even with the appearance of more complex fracture mechanisms, the statistical analysis showed that the main factor responsible for the improvement in the mechanical properties evaluated was the increase in fiber content and not the treatment with CaLS in an ultrasonic bath, since the results indicated that in both tests (Charpy and Izod) the TVF40-CaLS-UB composites, the product of the present study, always demonstrated an equal or inferior level in relation to TVF40-U and TVF40-CaLS-70°C, inferring that there was fiber embrittlement after surface modification. This weakening previously observed due to the decrease in fiber crystallinity, combined with the weak fiber/matrix compatibility power highlighted in the moisture absorption test, gave indications that the mechanical properties could be modest.

Although moderate impact resistance was observed, the reduced MFA highlights the potential of CaLS-treated fibers for load-bearing applications where rigidity and structural alignment are advantageous. The results suggest that, with continuous optimizations of the CaLS treatment applied to NLFs, such as increasing the modifying agent concentration and varying the sonication time, the developed composites can be efficiently targeted to meet applications with higher demands, durability and mechanical performance.

4. Conclusions

This pioneering study evaluated the chemical, structural, physical, and mechanical properties of Amazonian titica fibers (TVFs) treated with ultrasound-assisted calcium lignosulfonate (CaLS), as well as their epoxy matrix composites. The main results obtained were:

FTIR spectroscopy identified absorption bands associated with functional groups typical of lignocellulosic materials. The intensification of the bands at 2924 cm^{-1} and 1041 cm^{-1} was attributed to the addition of methoxyl and sulfonate groups, respectively.

The treatment of TVF with CaLS resulted in a 29.6% reduction in the crystallinity index of the fibers, attributed to the mechanical action of the ultrasonic bath. In addition, there was a 16.8% decrease in the microfibrillar angle (MFA),

reaching 6.61° , which may influence the overall properties of the fibers and their composites.

The water absorption test, carried out on the treated fiber composites, showed an absorption of 15.28%, 1.51 percentage points higher than that the untreated samples. The diffusion coefficient of the samples was measured at $D = 3.900 \times 10^{-4} (\text{mm}^2.\text{h}^{-1})$ and the parameter $K = 0.997$, indicating that the material was more prone to absorbing water and had a greater capacity for movement of molecules within the composite than those without any treatment. Nevertheless, these composites demonstrated better performance than several other polymer matrix composites reinforced with NLFs previously reported.

The Charpy and Izod impact tests were performed on samples containing 10–40 vol% of CaLS-treated fibers in an ultrasonic bath to evaluate their mechanical properties. Weibull statistical analysis indicated that composites with 30 and 40 vol% of treated fibers presented lower homogeneity, which was evidenced by the low β value in these samples. The parameter θ followed the same pattern of impact resistance results measured directly in the tests, while the statistical precision coefficient R^2 was shown to be within a statistically acceptable reliability range (> 0.83).

In the Charpy test, ANOVA followed by Tukey's test indicated that the TVF40-CaLS-UB group exhibited no significant difference compared to plain epoxy and TVF40-ST (40 vol% untreated). In contrast, in the Izod test, TVF40-CaLS-UB composites demonstrated significantly higher impact resistance than plain epoxy, but lower than TVF40-U.

SEM analysis of the fractured specimens showed that, although the samples with a higher fiber content treated in an ultrasonic bath (40 vol%) presented more complex fracture mechanisms, this was not enough to improve their mechanical properties compared to the untreated samples. This was evidenced by the strong presence of river marks in the samples and through statistical analyses. In fact, what drove the slight increase in impact resistance was the increase in the percentage of fibers and not the treatment applied.

Despite the obtained results and identified limitations, the reduction in MFA indicates potential for improving the mechanical properties of the composites. It should be considered that these tested materials may not be suitable for applications subjected to abrupt and dynamic loading, such as impact tests. However, they demonstrate viability for applications requiring intermediate mechanical performance and moisture resistance, suggesting their use in sectors such as civil construction and the furniture industry.

5. Future Work

As evidenced by the results, the present study exhibited certain limitations, particularly a slight reduction in the crystallinity index of the fibers following treatment, as well as a decrease in the Izod impact resistance of the composites reinforced with treated fibers compared to those reinforced with untreated fibers. To mitigate these adverse effects, it is recommended to conduct further experiments by varying treatment parameters such as CaLS concentration, sonication time, and the type of polymer matrix used.

6. References

- Elfaleh I, Abbassi F, Habibi M, Ahmad F, Guedri M, Nasri M, et al. A comprehensive review of natural fibers and their composites: an eco-friendly alternative to conventional materials. *Results Eng.* 2023;19:101271. <http://doi.org/10.1016/j.rineng.2023.101271>.
- Pothan LA, Oommen Z, Thomas S. Dynamic mechanical analysis of banana fiber reinforced polyester composites. *Compos Sci Technol.* 2023;63(2):283-93. [http://doi.org/10.1016/S0266-3538\(02\)00254-3](http://doi.org/10.1016/S0266-3538(02)00254-3).
- Thyaviahalli Giriappa YG, Mavinkere Rangappa S, Parameswaranpillai J, Siengchin S. Natural fibers as sustainable and renewable resource for development of eco-friendly composites: a comprehensive review. *Front Mater.* 2019;6:226. <http://doi.org/10.3389/fmats.2019.00226>.
- Karimah A, Ridho MR, Munawar SS, Adi DS, Damayanti R, Subiyanto B, et al. A review on natural fibers for development of eco-friendly bio-composite: characteristics, and utilizations. *J Mater Res Technol.* 2021;13:2442-58. <http://doi.org/10.1016/j.jmrt.2021.06.014>.
- Madueke CI, Mbah OM, Umunakwe R. A review on the limitations of natural fibers and natural fibre composites with emphasis on tensile strength using coir as a case study. *Polym Bull.* 2023;80(4):3489-506. <http://doi.org/10.1007/s00289-022-04241-y>.
- Mohd Bakhori SN, Hassan MZ, Mohd Bakhori N, Jamaludin KR, Ramlie F, Md Daud MY, et al. Physical, mechanical and perforation resistance of natural-synthetic fiber interply laminate hybrid composites. *Polymers (Basel).* 2022;14(7):1322. <http://doi.org/10.3390/polym14071322>.
- Balasubramanian M, Saravanan R. Exploring natural plant fiber choices and treatment methods for contemporary composites: a comprehensive review. *Results Eng.* 2024;24:103270. <https://doi.org/10.1016/j.rineng.2024.103270>.
- Paramathma BS, Sundaram M, Palani V, Raghunathan V, Dhillip JDJ, Khan A. Characterization of silane treated and untreated Citrullus lanatus fibers based eco-friendly automotive brake friction composites. *J Nat Fibers.* 2022;19(16):13273-87. <http://doi.org/10.1080/15440478.2022.2089431>.
- Raghunathan V, Ayyappan V, Dhillip JDJ, Sundarajan D, Rangappa SM, Siengchin S. Influence of alkali-treated and raw Zanthoxylum acanthopodium fibers on the mechanical, water resistance, and morphological behavior of polymeric composites for lightweight applications. *Biomass Convers Biorefin.* 2024;14(19):24345-57. <http://doi.org/10.1007/s13399-023-04240-7>.
- Raghunathan V, Sathyamoorthy G, Ayyappan V, Singaravelu DL, Rangappa SM, Siengchin S. Effective utilization of surface-processed/untreated Cardiospermum halicababum agro-waste fiber for automobile brake pads and its tribological performance. *Tribol Int.* 2024;197:109776. <http://doi.org/10.1016/j.triboint.2024.109776>.
- Raghunathan V, Dhillip JDJ, Subramanian G, Narasimhan H, Baskar C, Murugesan A, et al. Influence of chemical treatment on the physico-mechanical characteristics of natural fibers extracted from the barks of Vachellia farnesiana. *J Nat Fibers.* 2022;19(13):5065-75. <http://doi.org/10.1080/15440478.2021.1875353>.
- Tengsuthiwat J, Vinod A, Vijay R, Rangappa SM, Siengchin S. Characterization of novel natural cellulose fiber from Ficus macrocarpa bark for lightweight structural composite application and its effect on chemical treatment. *Heliyon.* 2024;10(9):e30442. <http://doi.org/10.1016/j.heliyon.2024.e30442>.
- Sheeba KRJ, Priya RK, Arunachalam KP, Avudaiappan S, Maureira-Carsalade N, Roco-Videla Á. Characterisation of sodium acetate treatment on acacia pennata natural fibres. *Polymers (Basel).* 2023;15(9):1996. <http://doi.org/10.3390/polym15091996>.
- Sanjay MR, Madhu P, Jawaid M, Senthamarakannan P, Senthil S, Pradeep S. Characterization and properties of natural fiber polymer composites: a comprehensive review. *J Clean Prod.* 2018;172:566-81. <http://doi.org/10.1016/j.jclepro.2017.10.101>.
- Al-Maharma AY, Al-Huniti N. Critical review of the parameters affecting the effectiveness of moisture absorption treatments used for natural composites. *J Compos Sci.* 2019;3(1):27. <http://doi.org/10.3390/jcs3010027>.
- Da Cunha JDSC, Nascimento LFC, Da Luz FS, Monteiro SN, Lemos MF, Da Silva CG, et al. Physical and mechanical characterization of titica vine (*Heteropsis flexuosa*) incorporated epoxy matrix composites. *Polymers (Basel).* 2021;13(23):4079. <http://doi.org/10.3390/polym13234079>.
- Raghunathan V, Gnanasekaran S, Ayyappan V, Devanathan LS, Mavinkere Rangappa S, Siengchin S. Sustainable characterization of brake pads using raw/silane-treated Mimosa pudica fibers for automobile applications. *Polym Compos.* 2024;45(11):10204-19. <http://doi.org/10.1002/pc.28467>.
- Valadez-Gonzalez A, Cervantes-Uc JM, Olayo RJIP, Herrera-Franco PJ. Effect of fiber surface treatment on the fiber-matrix bond strength of natural fiber reinforced composites. *Compos, Part B Eng.* 1999;30(3):309-20. [http://doi.org/10.1016/S1359-8368\(98\)00054-7](http://doi.org/10.1016/S1359-8368(98)00054-7).
- Meenakshi Reddy R, Mohana Krishnudu D, Madhusudhan Reddy B, Venkateshwar Reddy P. Effect of alkali treatment on mechanical properties of tpsi fiber reinforced polyester composites. In: *Emerging Trends in Mechanical Engineering: Select Proceedings of ICETME 2018; 2018; Singapore. Proceedings.* USA: Springer; 2019. p. 85-91.
- Reddy BM, Reddy RM, Reddy PV, Prashanth NNA, Bandhu D. Effect of alkali treatment on mechanical properties and morphology of the Balanites aegyptiaca composite. *Proc Inst Mech Eng, C J Mech Eng Sci.* 2024;238(11):5077-86. <http://doi.org/10.1177/09544062231217596>.
- Reddy BM, Mohana Reddy YV, Mohan Reddy BC, Reddy RM. Mechanical, morphological, and thermogravimetric analysis of alkali-treated Cordia-Dichotoma natural fiber composites. *J Nat Fibers.* 2020;17(5):759-68. <http://doi.org/10.1080/15440478.2018.1534183>.
- Reddy BM, Reddy YVM, Reddy BCM, Kumar GS, Reddy PV, Rao HR. A study on mechanical, structural, morphological, and thermal properties of raw and alkali treated Cordia dichotoma-polyester composite. *Polym Compos.* 2021;42(1):309-19. <http://doi.org/10.1002/pc.25826>.
- Maniraj J, Sahayaraj F, Giri J, Sathish T, Shaik MR. Enhancing performance of Prosopis juliflora fiber reinforced epoxy composites with silane treatment and Syzygium cumini filler. *J Mater Res Technol.* 2024;31:93-108. <http://doi.org/10.1016/j.jmrt.2024.06.058>.
- Xu Y, Fan Z, Li X, Yang S, Wang J, Zheng A, et al. Cooperative production of monophenolic chemicals and carbon adsorption materials from cascade pyrolysis of acid hydrolysis lignin. *Bioresour Technol.* 2024;399:130557. <http://doi.org/10.1016/j.biortech.2024.130557>.
- Rajesh M, Pitchaimani J. Mechanical characterization of natural fiber intra-ply fabric polymer composites: influence of chemical modifications. *J Reinf Plast Compos.* 2017;36(22):1651-64. <http://doi.org/10.1177/0731684417723084>.
- Oliveira F, Silva CG, Ramos LA, Frollini E. Phenolic and lignosulfonate-based matrices reinforced with untreated and lignosulfonate-treated sisal fibers. *Ind Crops Prod.* 2017;96:30-41. <http://doi.org/10.1016/j.indcrop.2016.11.027>.
- Romaní A, Garrote G, López F, Parajó JC. Eucalyptus globulus wood fractionation by autohydrolysis and organosolv delignification. *Bioresour Technol.* 2011;102(10):5896-904. <http://doi.org/10.1016/j.biortech.2011.02.070>.
- Doherty WO, Mousavioun P, Fellows CM. Value-adding to cellulosic ethanol: lignin polymers. *Ind Crops Prod.* 2011;33(2):259-76. <http://doi.org/10.1016/j.indcrop.2010.10.022>.

29. Ren H, Quan Y, Liu S, Hao J. Effectiveness of ultrasound (US) and slightly acidic electrolyzed water (SAEW) treatments for removing *Listeria monocytogenes* biofilms. *Ultrason Sonochem*. 2025;112:107190. <http://doi.org/10.1016/j.ultsonch.2024.107190>.
30. Ribeiro MP, de Mendonça Neuba L, da Silveira PHPM, da Luz FS, da Silva Figueiredo ABH, Monteiro SN, et al. Mechanical, thermal and ballistic performance of epoxy composites reinforced with Cannabis sativa hemp fabric. *J Mater Res Technol*. 2021;12:221-33. <http://doi.org/10.1016/j.jmrt.2021.02.064>.
31. Segal LGJMA, Creely JJ, Martin AE Jr, Conrad CM. An empirical method for estimating the degree of crystallinity of native cellulose using the X-ray diffractometer. *Text Res J*. 1959;29(10):786-94. <http://doi.org/10.1177/004051755902901003>.
32. Donaldson L. Microfibril angle: measurement, variation and relationships—a review. *IAWA J*. 2008;29(4):345-86. <http://doi.org/10.1163/22941932-90000192>.
33. Sarén MP, Serimaa R. Determination of microfibril angle distribution by X-ray diffraction. *Wood Sci Technol*. 2006;40(6):445-60. <http://doi.org/10.1007/s00226-005-0052-7>.
34. American Society for Testing and Materials. D570-98: standard test method for water absorption of plastics. West Conshohocken, PA, USA: American Society for Testing and Materials; 2018.
35. Espert A, Vilaplana F, Karlsson S. Comparison of water absorption in natural cellulosic fibres from wood and one-year crops in polypropylene composites and its influence on their mechanical properties. *Compos, Part A Appl Sci Manuf*. 2004;35(11):1267-76. <http://doi.org/10.1016/j.compositesa.2004.04.004>.
36. Megiatto JD Jr, Oliveira FB, Rosa DS, Gardrat C, Castellán A, Frollini E. Renewable resources as reinforcement of polymeric matrices: composites based on phenolic thermosets and chemically modified sisal fibers. *Macromol Biosci*. 2007;7(9-10):1121-31. <http://doi.org/10.1002/mabi.200700083>.
37. Osman EA, Vakhguel A, Sbarski I, Mutasher SA. Kenaf/ recycled jute natural fibers unsaturated polyester composites: water absorption/dimensional stability and mechanical properties. *Int J Comput Mater Sci Eng*. 2012;1(1):1250010. <http://doi.org/10.1142/S2047684112500108>.
38. American Society for Testing and Materials. D6110-18: standard test method for determining the charpy impact resistance of notched specimens of plastics. West Conshohocken, PA, USA: American Society for Testing and Materials; 2018.
39. American Society for Testing and Materials. D256-10: standard test methods for determining the izod pendulum impact resistance of plastics. West Conshohocken, PA, USA: American Society for Testing and Materials; 2000.
40. Cunha JSC, Nascimento LFC, Luz FSD, Garcia Filho FDC, Oliveira MS, Monteiro SN. Titica Vine Fiber (Heteropsis flexuosa): a hidden Amazon Fiber with potential applications as reinforcement in Polymer Matrix composites. *J Compos Sci*. 2022;6(9):251. <http://doi.org/10.3390/jcs6090251>.
41. Almeida LM, Da Silva ACR, Lopes FPD, Simonassi NT, Monteiro SN, Candido VS. Caranan fibers (Mauritiella armata) and new reinforcements of polyester composites with natural fibers functionalized with graphene oxide and their application potential. *J Mater Res Technol*. 2025;34:2232-52. <http://doi.org/10.1016/j.jmrt.2024.12.233>.
42. Monteiro SN, Margem FM, Margem JI, De Souza Martins LB, Oliveira CG, Oliveira MP. Infra-red spectroscopy analysis of malva fibers. *Mater Sci Forum*. 2014;775:255-60. <http://doi.org/10.4028/www.scientific.net/MSF.775-776.255>.
43. Albinante SR, Pacheco EB, Visconte LL, Tavares MI. Caracterização de fibras de bananeira e de coco por ressonância magnética nuclear de alta resolução no estado sólido. *Polímeros*. 2012;22(5):460-6. <http://doi.org/10.1590/S0104-14282012005000057>.
44. Li Z, Zhang X, Fa C, Zhang Y, Xiong J, Chen H. Investigation on characteristics and properties of bagasse fibers: performances of asphalt mixtures with bagasse fibers. *Constr Build Mater*. 2020;248:118648. <http://doi.org/10.1016/j.conbuildmat.2020.118648>.
45. Parre A, Karthikeyan B, Balaji A, Udhayasankar R. Investigation of chemical, thermal and morphological properties of untreated and NaOH treated banana fiber. *Mater Today Proc*. 2020;22:347-52. <http://doi.org/10.1016/j.matpr.2019.06.655>.
46. Li Z, Ge Y. Extraction of lignin from sugar cane bagasse and its modification into a high performance dispersant for pesticide formulations. *J Braz Chem Soc*. 2011;22(10):1866-71. <http://doi.org/10.1590/S0103-50532011001000006>.
47. Bufalino L, De Sena Neto AR, Tonoli GHD, De Souza Fonseca A, Costa TG, Marconcini JM, et al. How the chemical nature of Brazilian hardwoods affects nanofibrillation of cellulose fibers and film optical quality. *Cellulose*. 2015;22(6):3657-72. <http://doi.org/10.1007/s10570-015-0771-3>.
48. Vinod A, Vijay R, Singaravelu DL, Sanjay MR, Siengchin S, Moure MM. Characterization of untreated and alkali treated natural fibers extracted from the stem of Catharanthus roseus. *Mater Res Express*. 2019;6(8):085406. <http://doi.org/10.1088/2053-1591/ab22d9>.
49. Boukir A, Fellak S, Doumenq P. Structural characterization of Argania spinosa Moroccan wooden artifacts during natural degradation progress using infrared spectroscopy (ATR-FTIR) and X-Ray diffraction (XRD). *Heliyon*. 2019;5(9):e02477. <http://doi.org/10.1016/j.heliyon.2019.e02477>.
50. Vidal C, Carrillo-Varela I, Reyes-Contreras P, Gutierrez L, Mendonça RT. Sulfomethylation of radiata pine kraft lignin and its use as a molybdenite depressant in selective chalcocopyrite-molybdenite separation by flotation. *BioResources*. 2021;16(3):3. <http://doi.org/10.15376/biores.16.3.5646-5666>.
51. Ibrahim MM, Dufresne A, El-Zawawy WK, Agblevor FA. Banana fibers and microfibrils as lignocellulosic reinforcements in polymer composites. *Carbohydr Polym*. 2010;81(4):811-9. <http://doi.org/10.1016/j.carbpol.2010.03.057>.
52. Duan X, Wang X, Chen J, Liu G, Liu Y. Structural properties and antioxidant activities of lignins isolated from sequential two-step formosolv fractionation. *RSC Advances*. 2022;12(37):24242-51. <http://doi.org/10.1039/D2RA02085H>.
53. Flannigan DJ, Hopkins SD, Suslick KS. Sonochemistry and sonoluminescence in ionic liquids, molten salts, and concentrated electrolyte solutions. *J Organomet Chem*. 2025;690(15):3513-7. <http://doi.org/10.1016/j.jorgchem.2005.04.024>.
54. Mason TJ, Riera E, Vercet A, Lopez-Buesa P. Application of ultrasound. In: Sun DW, editor. *Emerging technologies for food processing*. Cambridge: Academic Press; 2005. p. 323-51.
55. Hagenson LC, Doraiswamy LK. Comparison of the effects of ultrasound and mechanical agitation on a reacting solid-liquid system. *Chem Eng Sci*. 1998;53(1):131-48. [http://doi.org/10.1016/S0009-2509\(97\)00193-0](http://doi.org/10.1016/S0009-2509(97)00193-0).
56. Mwaikambo LY, Ansell MP. Chemical modification of hemp, sisal, jute, and kapok fibers by alkalization. *J Appl Polym Sci*. 2002;84(12):2222-34. <http://doi.org/10.1002/app.10460>.
57. Bekraoui N, El Qoubaa Z, Chouiyakh H, Faqir M, Essadiqi E. The influence of structural and chemical parameters on mechanical properties of natural fibers: a statistical exploratory analysis. *J Polym Eng*. 2022;42(5):385-94. <http://doi.org/10.1515/polyeng-2021-0241>.
58. Petroudy SD. Physical and mechanical properties of natural fibers. In: Fan M, Fu F, editors. *Advanced high strength natural fibre composites in construction*. USA: Elsevier; 2017. p. 59-83.
59. Neuba LDM, Junio RFP, Souza AT, Ribeiro MP, Da Silveira PHPM, Da Silva TT, et al. Mechanical properties, critical length, and interfacial strength of seven-islands-sedge fibers (Cyperus malaccensis) for possible epoxy matrix reinforcement. *Polymers (Basel)*. 2022;14(18):3807. <http://doi.org/10.3390/polym14183807>.
60. Suryanto H, Marsyahyo E, Irawan YS, Soenoko R. Morphology, structure, and mechanical properties of natural cellulose fiber from mendong grass (Fimbristylis globulosa). *J Nat Fibers*.

- 2014;11(4):333-51. <http://doi.org/10.1080/15440478.2013.879087>.
61. Silva TTD, Silveira PHPMD, Ribeiro MP, Lemos MF, Da Silva AP, Monteiro SN, et al. Thermal and chemical characterization of kenaf fiber (*Hibiscus cannabinus*) reinforced epoxy matrix composites. *Polymers (Basel)*. 2021;13(12):2016. <http://doi.org/10.3390/polym13122016>.
 62. Sheeba KJ, Priya RK, Arunachalam KP, Avudaiappan S, Flores ES, Kozlov P. Enhancing structural, thermal, and mechanical properties of *Acacia pennata* natural fibers through benzoyl chloride treatment for construction applications. *Case Stud Construct Mater*. 2023;19:e02443. <http://doi.org/10.1016/j.cscm.2023.e02443>.
 63. Hyness NRJ, Vignesh N, Senthamarakannan P, Saravanakumar S, Sanjay M. Characterization of new natural cellulosic fiber from heteropogon contortus plant. *J Nat Fibers*. 2018;15(1):146-53. <http://doi.org/10.1080/15440478.2017.1321516>.
 64. Manimaran P, Prithiviraj M, Saravanakumar S, Arthanarieswaran V, Senthamarakannan P. Physicochemical, tensile, and thermal characterization of new natural cellulosic fibers from the stems of *Sida cordifolia*. *J Nat Fibers*. 2018;15(6):860-9. <http://doi.org/10.1080/15440478.2017.1376301>.
 65. Azwa ZN, Yousif BF, Manalo AC, Karunasena W. A review on the degradability of polymeric composites based on natural fibres. *Mater Des*. 2013;47:424-42. <http://doi.org/10.1016/j.matdes.2012.11.025>.
 66. Da Silveira PHPM, Santos MCCD, Chaves YS, Ribeiro MP, Marchi BZ, Monteiro SN, et al. Characterization of thermo-mechanical and chemical properties of polypropylene/hemp fiber biocomposites: impact of maleic anhydride compatibilizer and fiber content. *Polymers (Basel)*. 2023;15(15):3271. <http://doi.org/10.3390/polym15153271>.
 67. Gerald Arul Selvan M, Athijayamani A. Mechanical properties of fragrant screwpine fiber reinforced unsaturated polyester composite: effect of fiber length, fiber treatment and water absorption. *Fibers Polym*. 2016;17(1):104-16. <http://doi.org/10.1007/s12221-016-5593-x>.
 68. Uma Devi L, Joseph K, Manikandan Nair KC, Thomas S. Ageing studies of pineapple leaf fiber–reinforced polyester composites. *J Appl Polym Sci*. 2004;94(2):503-10. <http://doi.org/10.1002/app.20924>.
 69. Dos Santos Carneiro da Cunha J, De Oliveira Neto HE, Giacon VM, Manzato L, Da Silva CG. Study on mechanical and thermal properties of Amazon fibers on the polymeric biocomposites: malva and tucum. *Fibers Polym*. 2021;22(11):3203-11. <http://doi.org/10.1007/s12221-021-0843-y>.
 70. Ferreira ADS, Lopes FPD, Monteiro SN, Satyanarayana KG. Charpy impact resistance of alkali treated curaua reinforced polyester composites. *Materia (Rio J)*. 2010;15(2):131-7. <http://doi.org/10.1590/S1517-70762010000200007>.
 71. Robledo-Ortiz JR, González-López ME, Rodrigue D, Gutiérrez-Ruiz JF, Prezas-Lara F, Pérez-Fonseca AA. Improving the compatibility and mechanical properties of natural fibers/green polyethylene biocomposites produced by rotational molding. *J Polym Environ*. 2020;28(3):1040-9. <http://doi.org/10.1007/s10924-020-01667-1>.
 72. Almeida LM, Da Silva ACR, Lopes FPD, Simonassi NT, Monteiro SN, Candido VS. Caranan fibers (*Mauritiella armata*) and new reinforcements of polyester composites with natural fibers functionalized with graphene oxide and their application potential. *J Mater Res Technol*. 2025;34:2232-52. <http://doi.org/10.1016/j.jmrt.2024.12.233>.
 73. Senthilkumar K, Chandrasekar M, Alothman OY, Fouad H, Jawaid M, Azeem MA. Flexural, impact and dynamic mechanical analysis of hybrid composites: olive tree leaves powder/pineapple leaf fibre/epoxy matrix. *J Mater Res Technol*. 2022;21:4241-52. <http://doi.org/10.1016/j.jmrt.2022.11.036>.

Data Availability

All the data set supporting the results of this study has been published in the article itself.